The Primary Electroviscous Effect of Rigid Polyions of Arbitrary Shape and Charge Distribution

Stuart A. Allison

Department of Chemistry, Georgia State University, Atlanta, Georgia 30303

Received February 19, 1998; Revised Manuscript Received May 7, 1998

ABSTRACT: The viscosity of a dilute suspension of charged rigid particles exceeds that of a suspension of identical, but uncharged particles, and this is called the primary electroviscous effect. This excess viscosity arises as a result of the distortion of the ion atmosphere surrounding the polyion due to the fluid shear field in which it is placed. Consequently, any theory of the primary electroviscous effect must account for this distortion. Booth (*Proc. Roy. Soc. (London)* **1950**, *203A*, 533) and later Sherwood (*J. Fluid Mech.* **1980**, *101*, 609) achieved this for a spherical polyion of uniform equilibrium surface potential by solving the coupled (low Reynold's number) Navier−Stokes, Poisson, and ion transport equations. The primary objective of the present work is to extend this approach to rigid model polyions of arbitrary shape and charge distribution. The coupled transport equations are solved by an iterative boundary element (BE) procedure applied previously to the closely related problem of electrophoresis (Allison, S. A. *Macromolecules* **1996**, *29*, 7391). In test cases on spheres containing single central charges, the BE results are found to be in very good agreement with Sherwood. The BE approach is then applied to spherical polyions containing noncentrosymmetric charge distributions as well as short (20−40 base pair) DNA models in the monovalent salt range 0.005−0.6 M. For the DNA fragments, the primary electroviscous effect ranges from about 2% to 30% (40 bp) or 45% (20bp) as the KCl concentration is reduced from 0.6 to 0.005 M, respectively. Substantially larger effects are predicted if the monovalent salt is Tris−acetate, and this is due primarily to the lower mobility of the Tris counterion relative to K^+. A secondary objective is to make contact between the BE approach and "bead methods", which have been successfully used in modeling the viscosity of rigid, but uncharged macromolecules of arbitrary shape.

Introduction

A long recognized but still poorly understood problem concerns the effect of charge on the viscosity of a suspension of biomolecules, polyelectrolytes, or colloid particles.[1−4] It has proven convenient to distinguish three types of interactions that give rise to what have collectively come to be called electroviscous effects. Consider first a solution of rigid charged particles sufficiently dilute so that the intrinsic viscosity is independent, or nearly so, on particle concentration. When this solution is placed in a shear field, the ion atmosphere around each particle is distorted and this distortion produces additional stresses on the bulk solution, thereby increasing the viscosity. This is called the primary electroviscous effect. For a more concentrated solution, particle−particle interactions become important and this gives rise to secondary electroviscous effects.[2] These secondary effects can be substantial for high molecular weight polyelectrolytes at low salt.[5] Flexible polyelectrolytes may exhibit tertiary electroviscous effects in which case the viscosity depends on polymer conformation and this, in turn, varies with salt concentration and possibly shear rate. As the salt concentration is increased in a suspension of flexible linear polyelectrolytes, for example, the average chain conformation contracts as electrostatic repulsions are screened.[6] This contraction leads to a reduction in viscosity. The purpose of the present work shall be an analysis of the primary electroviscous effect where we model the macromolecule as a rigid particle in a fluid sufficiently dilute so that particle−particle interactions can be ignored.

Viscosity theory of dilute *uncharged* macromolecules is extensive and well developed. Since this is not the subject of primary focus in the present work, only a few of the major contributions shall be cited here. Einstein first solved the problem for spheres,[7] and a number of investigators extended this to prolate and oblate ellipsoids.[8−10] Kirkwood and Riseman[11] formulated a model to interpret the intrinsic viscosity of long, flexible, uncharged polymers. A key idea of Kirkwood and Riseman was to model the polymer as an array of subunits that act as centers of frictional resistance. This idea proved very useful later in modeling the intrinsic viscosity of rigid macromolecules of arbitrary shape as arrays of spherical beads.[12−14] At the continuum level, in which the macromolecule is modeled as a rigid body immersed in a uniform, low-shear, Newtonian fluid, the intrinsic viscosity can be numerically calculated for any shape using these bead methods.[14,15]

Viscosity theory of charged macromolecules is substantially more complicated due to the fact that the motion of the fluid in a shear field distorts the ion atmosphere around the macromolecule and this alters the viscosity. As in the theory for uncharged particles/macromolecules, the fluid around the macromolecule is modeled as a uniform, structureless continuum. Several additional approximations are made when treating the viscosity of charged macromolecules. First of all, the ion atmosphere is modeled as a continuum of point charges and it is assumed that the local charge density and steady-state electrodynamic potential are related to each other through Poisson's equation. An additional continuum equation is also used to balance the steady state transport of co- and counterions in the vicinity of the macromolecule due to the combined effects of convection, diffusion, and direct forces. To account for the distortion of the ion atmosphere, or ion relaxation, it becomes necessary to simultaneously solve five or more coupled equations: linearized Navier−Stokes and

S0024-9297(98)00250-2 CCC: $15.00
Published on Web 06/19/1998

solvent incompressibility (to obtain the fluid velocity), Poisson (for the electrodynamic potential), and ion transport (for each ion distribution). At the present time, only a spherical particle containing a centrosymmetric charge distribution has been sucessfully treated.[16−19] The most recent work by Sherwood[19] is the most general. The complicating feature of "ion relaxation" seen in viscosity also appears in other electrokinetic phenomena such as electrophoresis.[20] Over the past few years, boundary element (BE) methods have been developed and used to model the electrophoretic mobility of rigid model macromolecules of arbitrary shape and charge distribution and account can be taken of ion relaxation.[21−23] With slight modification, it is straightforward to apply the BE methodology to the viscosity of charged macromolecules and that is the primary objective of the present work. Conceptually, the BE approach is quite similar to the bead methods applied to uncharged macromolecules 20 years ago.[12−15] Instead of modeling the particle as a bead array, however, the particle is modeled as a closed surface made up of an array of triangular plates. Once a particular charge distribution and surface model are defined, the Navier−Stokes, Poisson, and ion transport equations are solved by an iterative, BE procedure.[21−23]

The outline of this paper is as follows. In the next section, we outline the procedures used to calculate ion relaxation in a shear field and define those quantities needed to compute viscosities. The following section explains how a macroscopic viscosity of a suspension of dilute particles is computed from a BE calculation. This is followed by an applications section where we first look at model macromolecules that can be compared with existing theory (uncharged prolate ellipsoids and charged spheres), and then at a number of more complicated model systems. These include spherical polyions containing noncentrosymmetric charge distributions and capped cylinder models for short DNA fragments in the size range of 20−40 base pairs in length. The DNA studies are carried out over a range of monovalent salt concentrations to see how salt influences the primary electroviscous effect. Because of similarities between the BE approach applied here and bead methods,[11−15] we felt it was worthwhile to explore the correspondence between the two approaches for the special case of uncharged model macromolecules. However, since uncharged particles are not the primary focus of the present work, this question is relegated to Appendix B. We end with a brief summary of this work.

Outline of the Problem and Method of Solution

When a macroion is placed in a shear field as is done in a viscosity experiment, the coion and counterion atmosphere surrounding the macroion is distorted. It is this distortion, or "ion relaxation", that raises the viscosity of the suspension of macroions above that expected of a suspension of identical, but uncharged, particles. This effect is called the primary electroviscous effect and its solution requires that proper account be taken of ion relaxation that arises in response to an imposed external shear field. As in closely related work in electrophoresis,[20−23] an important quantity required is the external force per unit volume, $\mathbf{s}(\mathbf{y})$, exerted on the fluid at position $\mathbf{y}$. It shall be assumed that $\mathbf{s}$ arises from the various electrostatic interactions that are present. If Λ denotes the total electrodynamic potential and ρ the local charge density, then

$$\mathbf{s}(\mathbf{y}) = -\rho(\mathbf{y})\nabla\Lambda(\mathbf{y}) \tag{1}$$

Outside the macroion, ρ is treated as a continuum and can be written

$$\rho(\mathbf{y}) = q\sum_{\alpha} z_\alpha n_\alpha(\mathbf{y}) \tag{2}$$

where q is the protonic charge, z_α is the valence of ion α, and n_α is the local ion concentration. It is convenient to break Λ into the potential of a stationary polyion in the absence of a shear field, Λ_0, and a perturbation potential, ψ, which arises as a consequence of ion relaxation.

$$\Lambda(\mathbf{y}) = \Lambda_0(\mathbf{y}) + \psi(\mathbf{y}) \tag{3}$$

The potential and charge density are related through Poisson's equation

$$\nabla\cdot(\epsilon(\mathbf{y})\nabla\Lambda(\mathbf{y})) = -4\pi\rho(\mathbf{y}) \tag{4}$$

where ϵ is the local dielectric constant, which in this work is set to 2 inside the macroion and 78 outside. As discussed previously,[21,24] additional potentials, Φ_α, must be introduced to account for the departure of n_α from its equilibrium value, $n_{\alpha 0}$:

$$n_\alpha(\mathbf{y}) = n_{\alpha 0}(\mathbf{y})\mathrm{e}^{-\beta z_\alpha q(\psi(\mathbf{y})+\Phi_\alpha(\mathbf{y}))} \tag{5}$$

$$n_{\alpha 0}(\mathbf{y}) = c_{\alpha 0}\mathrm{e}^{-\beta z_\alpha q\Lambda_0(\mathbf{y})} \tag{6}$$

where $\beta = 1/k_\mathrm{B}T$ and $c_{\alpha 0}$ is the ambient concentration of ion α. As in previous work on electrophoresis, the analysis shall be restricted to linear terms in the imposed perturbation, which in the present application is the shear field. Consequently, eq 5 is approximated with

$$n_\alpha(\mathbf{y}) = n_{\alpha 0}(\mathbf{y})[1 - \beta z_\alpha q(\psi(\mathbf{y})+\Phi_\alpha(\mathbf{y}))] \tag{7}$$

It should be emphasized, however, that although only linear terms in ψ, Φ_α, and the fluid velocity field, $\mathbf{v}$, are retained, nonlinear terms in Λ_0 are retained. In the absence of any perturbation, eq 4 reduces to the full Poisson−Boltzmann equation

$$\nabla\cdot(\epsilon(\mathbf{y})\nabla\Lambda_0(\mathbf{y})) = -4\pi\rho_0(\mathbf{y}) \tag{8}$$

and outside the macroion

$$\rho_0(\mathbf{y}) = q\sum_{\alpha} c_{\alpha 0} z_\alpha \mathrm{e}^{-\beta q z_\alpha \Lambda_0(\mathbf{y})} \tag{9}$$

As described elsewhere,[21−23] Λ_0 is solved by a nonlinear boundary element procedure similar to that employed by Zhou.[25] The macroion surface is subdivided into N triangular plates and the assumption is made that the electrostatic potential and normal derivative are constant over a given plate. It is also necessary to discretize the space surrounding the polyion to account for the contribution of the ion atmosphere (or at least the nonlinear Poisson−Boltzmann source terms) to the electrostatic potential. This discretization is also required to solve for the other potential problems as well as $\mathbf{v}$. In the present work, the space sorrounding the macroion is subdivided into J shells (typically 50) and each shell, in turn, is divided into N volume elements. The thickness of the shells increases as one moves away

from the surface such that κd typically equals 8−24 where κ is the Debye−Huckel screening parameter and d is the distance of the furthest shell from the macroion's surface. It is only necessary to solve for Λ_0 once, and it along with $\nabla\Lambda_0$ are saved for future use. In the absence of relaxation, it is straightforward to show that the external force per unit volume, $\mathbf{s}_0$, can be written

$$s_0(\mathbf{y}) = k_B T \sum_\alpha \nabla n_{\alpha 0}(\mathbf{y}) = \nabla \pi_0(\mathbf{y}) \tag{10}$$

where

$$\pi(\mathbf{y}) = k_B T \sum_\alpha n_\alpha(\mathbf{y}) \tag{11}$$

is the osmotic pressure within an additive constant and the "0" subscript denotes the equilibrium value.

The potentials ψ and Φ_α are also solved by BE procedures and can, through linearization, be put in the general form[21]

$$\nabla^2 \phi(\mathbf{y}) = f(\mathbf{y}) \tag{12}$$

where f is a source term. In general, these source terms contain unknown quantities that we are seeking to obtain. For Φ_α, for example,

$$f_\alpha(\mathbf{y}) = \left[\frac{1}{D_\alpha}\mathbf{v}(\mathbf{y}) + \beta z_\alpha q \nabla\Phi_\alpha(\mathbf{y})\right]\cdot\nabla\Lambda_0(\mathbf{y}) \tag{13}$$

where D_α is the diffusion constant of ion α, and $\mathbf{v}(\mathbf{y})$ is the local fluid velocity. (In applications such as electrophoresis, there is an additional term due to an external electric field.) At the beginning of the calculation, we do not know f_α since $\mathbf{v}$ and Φ_α are unknown. However, we can use previous estimates of $\mathbf{v}$ and Φ_α to approximate f_α and then use these in a BE solution of eq 12 to obtain a better estimate of Φ_α. An analogous strategy is applied to $\mathbf{v}$ (see below) and ψ. This whole approach is iterated until all quantities converge. To begin, it is assumed that ion relaxation is negligible so ψ and Φ_α can be set to zero.

To determine $\mathbf{v}$, the fluid sorrounding the macroion is treated as an incompressible continuum and the linearized Navier−Stokes and solvent incompressibility equations

$$\eta_0\nabla^2\mathbf{v}(\mathbf{y}) - \nabla p(\mathbf{y}) = -\mathbf{s}(\mathbf{y}) \tag{14}$$

$$\nabla\cdot\mathbf{v}(\mathbf{y}) = 0 \tag{15}$$

must be solved subject to the appropriate boundary conditions for the fluid velocity at the macroion surface and far away from it. Consider a rigid macroion in a pure shear field defined by

$$\mathbf{v}_0(\mathbf{y}) = \frac{1}{2}\boldsymbol{E}\cdot(\mathbf{y} - \mathbf{c}) \tag{16}$$

where $\mathbf{E}$ is a symmetric and traceless second rank tensor, and $\mathbf{c}$ is a constant, but arbitrary, position vector. Then the velocity field at field point $\mathbf{y}$ in the surrounding fluid is given by[26−28]

$$\mathbf{v}(\mathbf{y}) = \mathbf{v}_0(\mathbf{y}) - \int_{S_p} \boldsymbol{U}(\mathbf{y},\mathbf{x})\cdot\mathbf{w}(\mathbf{x})\, dS_x - \int_\Omega \boldsymbol{U}(\mathbf{y},\mathbf{x})\cdot\mathbf{s}(\mathbf{x})\, dV_x \tag{17}$$

where S_p represents the macroion surface, Ω the volume external to the polyion, $\mathbf{w}$ represents the hydrodynamic stress force per unit area on the polyion, and

$$\boldsymbol{U}(\mathbf{x},\mathbf{y}) = -\frac{1}{8\pi\eta_0 r}[\boldsymbol{I} + \boldsymbol{R}(\mathbf{x},\mathbf{y})]$$

$$[\boldsymbol{R}(\mathbf{x},\mathbf{y})]_{ij} = \frac{\mathbf{r}_i\mathbf{r}_j}{r^2} \tag{18}$$

where $\mathbf{r} = \mathbf{y} - \mathbf{x}$, $r = |\mathbf{r}|$, and $\mathbf{I}$ is the 3×3 identity matrix. Equation 17 is derived in a number of texts under limiting special conditions.[26,27] Now discretize the surface/volume as discussed before and define

$$\boldsymbol{U}_{ij} = \frac{1}{A_j}\int_{S_j} \boldsymbol{U}(\mathbf{y}_i,\mathbf{x})\, dS_x \tag{19}$$

$$\boldsymbol{Q}_{ik} = \frac{1}{V_k}\int_{V_k} \boldsymbol{U}(\mathbf{y}_i,\mathbf{x})\, dV_x \tag{20}$$

$$\mathbf{w}_j = A_j\mathbf{w}(\mathbf{y}_i) \tag{21}$$

$$\mathbf{s}_k = V_k\mathbf{s}(\mathbf{y}_k) \tag{22}$$

where $\mathbf{y}_i$ and $\mathbf{y}_j$ are points on the macroion surface, $\mathbf{y}_k$ is a point in the fluid volume, and A_j and V_k represent the area and volume of discrete elements. At point $\mathbf{y}_i$ (on the surface), eq 17 becomes

$$\mathbf{h}_i = \sum_j \boldsymbol{U}_{ij}\cdot\mathbf{w}_j \tag{23}$$

$$\mathbf{h}_i = \mathbf{v}_{i0} - \mathbf{v}_i - \sum_k \boldsymbol{Q}_{ik}\cdot\mathbf{s}_k \tag{24}$$

From boundary conditions, we know $\mathbf{v}_{i0}$ and $\mathbf{v}_i$. Also, it shall be assumed that $\mathbf{s}_k$ is known or at least estimated in advance so $\mathbf{h}_i$ is known. It is straightforward to construct a $3N \times 3N$ supermatrix, $\mathbf{U}$, from the N^2 individual $\mathbf{U}_{ij}$ matrixes with the ijth 3×3 submatrix of $\mathbf{U}$ corresponding to $\mathbf{U}_{ij}$. Then, the inverse of $\mathbf{U}$, $\mathbf{S} = \mathbf{U}^{-1}$, is constructed. Identify the ijth 3×3 submatrix of $\mathbf{S}$ as $\mathbf{S}_{ij}$. The hydrodynamic stress forces are then

$$\mathbf{w}_i = \sum_j \boldsymbol{S}_{ij}\cdot\mathbf{h}_j \tag{25}$$

Once the $\mathbf{w}_i$'s are computed, the velocity field anywhere in the fluid can be computed by following eq 17.

In computing the velocity field, it is convenient to introduce auxiliary forces, $\mathbf{s}'$, defined by[21,24]

$$\mathbf{s}'(\mathbf{y}) = \mathbf{s}(\mathbf{y}) - \nabla\pi(\mathbf{y}) \tag{26}$$

where π is the osmotic pressure given by eq 11. As shown by O'Brien and White,[24] the osmotic pressure term does not contribute to the velocity field even though it may be large. In other words, solving eqs 14 and 15 for velocity field $\mathbf{v}'$ with $\mathbf{s}'$ replacing $\mathbf{s}$ gives exactly the same velocity field, $\mathbf{v}$, provided both velocity fields are subjected to the same boundary conditions on the macroion surface and far away from it. In the absence of ion relaxation, $\mathbf{s}' = \mathbf{0}$. When, however, $\mathbf{s}'$ replaces $\mathbf{s}$, the actual hydrodynamic stress forces, $\mathbf{w}$, must be replaced with $\mathbf{w}'$. It is not difficult to show that

$$\mathbf{w}'(\mathbf{y}) = \mathbf{w}(\mathbf{y}) - \pi(\mathbf{y})\,\mathbf{n}(\mathbf{y}) \tag{27}$$

where **n** is the local outward normal to the particle surface. Physically, the **w**′ represent the hydrodynamic stress forces on a polyion with the same boundary conditions on the velocity field as the actual problem but with **s** replaced with **s**′.

Relation to Viscosity

It shall be assumed we have a dilute solution of "particles" placed in a shear field. In some convenient laboratory frame of reference, the macroscopic fluid velocity, $\mathbf{v}_0'(\mathbf{y})$, at point **y** is given by

$$\mathbf{v}_0'(\mathbf{y}) = \gamma(\mathbf{y}\cdot\mathbf{e}_b)\mathbf{e}_a \tag{28}$$

where γ is the shear gradient, $\mathbf{e}_a$ is a unit vector along the flow direction, and $\mathbf{e}_b$ (assumed to be perpendicular to $\mathbf{e}_a$) is a unit vector in the direction of greatest shear. In a Zimm−Crothers viscometer,[29] for example, the solution is placed in a narrow gap between two concentric cylinders that rotate relative to each other. In this case, $\mathbf{e}_b$ is directed outward along the local normal to the inner cylinder surface and $\mathbf{e}_a$ is directed along the tangent to the inner cylinder surface. The solution viscosity, η, is related to the stress tensor, $\boldsymbol{\sigma}$, by the relation

$$\boldsymbol{\sigma}_{ab} = \mathbf{e}_a\cdot\boldsymbol{\sigma}\cdot e_b = \eta\gamma \tag{29}$$

Let η_0 and $\boldsymbol{\sigma}_0$ denote the viscosity and stress tensor in the absence of any particles. It is well-known that the presence of particles in the fluid increases the viscosity of the solution. It was Einstein[7] who first solved the problem for a solution of uncharged spherical particles, and other investigators have expanded upon Einstein's work.[8−15] Consider a monodisperse solution of particles and assume that the solution is dilute enough so that overlap between the ion atmospheres of different particles can be ignored to a good approximation. The macroscopic excess stress, $\boldsymbol{\sigma}^e = \boldsymbol{\sigma} - \boldsymbol{\sigma}_0$, can be related to single particle averages using an equation originally derived by Batchelor[30] for uncharged particles and extended by Russel[31] to include charge effects

$$\boldsymbol{\sigma}^e/c = -\langle\eta_0\int_{S_p}(\boldsymbol{v}\boldsymbol{n} + \boldsymbol{n}\boldsymbol{v})\,dS_y + \int_{S_p}\boldsymbol{w}\boldsymbol{y}\,dS_y + \int_\Omega \boldsymbol{s}\boldsymbol{y}\,dV_y\rangle \tag{30}$$

where c is the number concentration of particles or polyions, **n** is the local outward normal to the particle surface, and brackets ($\langle\,\rangle$) denote averaging over all possible particle positions and orientations. The total force on the particle, $\mathbf{z}_t$, is given by[28]

$$\mathbf{z}_t = -\int_{S_p}\mathbf{w}(\mathbf{y})\,dS_y - \int_\Omega \mathbf{s}(\mathbf{y})\,dS_y \tag{31}$$

and this force vanishes under steady-state conditions. For a rigid particle, the first term on the right-hand side (rhs) of eq 30 vanishes. It is useful to define a dimensionless quantity, ξ, by the relation

$$\xi = \lim_{c\to 0}\frac{1}{cV_p}\left(\frac{\eta}{\eta_0} - 1\right) \tag{32}$$

where V_p is the particle volume. For an uncharged sphere, $\xi = 2.5$ as derived by Einstein.[7] Other investigators[8−10] solved the problem for uncharged prolate and oblate ellipsoids and the resulting ξ's are presented in tabular[32] and graphical[32,33] form in a number of popular texts. The intrinsic viscosity, $[\eta]$, is closely related to ξ and is defined

$$[\eta] = \lim_{c'\to 0}\frac{1}{c'}\left(\frac{\eta}{\eta_0} - 1\right) \tag{33}$$

where c' is a weight concentration of the added particle. It is straightforward to show

$$[\eta] = \frac{N_{Av}V_p}{M}\xi \tag{34}$$

where N_{Av} is Avogadro's number and M is the molecular weight of the particle. From eqs 29−32 we obtain

$$\xi = -\frac{1}{\eta_0\gamma V_p}\langle\int_{S_p}\mathbf{w}_a(\mathbf{y}-\mathbf{c})_b\,dS_y + \int_\Omega \mathbf{s}_a(\mathbf{y}-\mathbf{c})_b\,dV_y\rangle \tag{35}$$

where a and b denote vector components along $\mathbf{e}_a$ and $\mathbf{e}_b$, respectively, and **c** is an arbitrary position vector. The inclusion of **c** in eq 36 is allowed by the fact that the steady-state total force on the particle vanishes according to eq 31.

Placing a particle in a macroscopic shear field given by eq 28 alters the fluid velocity, **v**′, near the particle as described by eq 17. In the shear field, the particle will translate as well as rotate. At point $\mathbf{y}_i$ on the particle surface

$$\mathbf{v}'(\mathbf{y}_i) = \gamma(\mathbf{d}\cdot\mathbf{e}_b)\mathbf{e}_a + \frac{1}{2}\gamma(\mathbf{y}_i - \mathbf{d})\times\mathbf{e}_c \tag{36}$$

where **d** denotes the center of rotation of the particle in some convenient lab frame, Σ, and $\mathbf{e}_c = \mathbf{e}_a\times\mathbf{e}_b$. It is convenient to decompose $\mathbf{v}_0'(\mathbf{y})$ into translational ($\mathbf{v}_0^t$), rotational ($\mathbf{v}_0^r(\mathbf{y})$), and deformational ($\mathbf{v}_0(\mathbf{y})$) terms

$$\begin{aligned}\mathbf{v}_0'(\mathbf{y}) &= \mathbf{v}_0^t + \mathbf{v}_0^r(\mathbf{y}) + \mathbf{v}_0(\mathbf{y})\\ &= \gamma(\mathbf{d}\cdot\mathbf{e}_b)\mathbf{e}_a + \frac{1}{2}\gamma(\mathbf{y}-\mathbf{d})\times\mathbf{e}_c + \frac{1}{2}\boldsymbol{E}\cdot(\mathbf{y}-\mathbf{d})\end{aligned} \tag{37}$$

and the ij component of **E** is

$$E_{ij} = \gamma(e_{ai}e_{bj} + e_{aj}e_{bi}) \tag{38}$$

If we also define

$$\mathbf{v}(\mathbf{y}) = \mathbf{v}'(\mathbf{y}) - \mathbf{v}_0^t - \mathbf{v}_0^r(\mathbf{y}) \tag{39}$$

then

$$\mathbf{v}(\mathbf{y}) = \mathbf{v}_0(\mathbf{y}) - \int_{S_p}\boldsymbol{U}(\mathbf{y},\mathbf{x})\cdot\mathbf{w}(\mathbf{x})\,dS_x - \int_\Omega \boldsymbol{U}(\mathbf{y},\mathbf{x})\cdot\mathbf{s}(\mathbf{x})\,dV_x \tag{40}$$

and for points on the particle surface, we now have $\mathbf{v}(\mathbf{y}_i) = \mathbf{0}$.

At this point, the problem is straightforward for a spherical particle containing a centrosymmetric charge distribution. The center of rotation, **d**, corresponds to the center of the particle and because of the high degree of symmetry, it is not necessary to average over particle

orientations. In this case we can choose a simple shear field such as $\mathbf{e}_a$ and $\mathbf{e}_b$ lying along x and y axes of the lab frame. The boundary element (BE) procedure is then carried out to determine the ion relaxation and the **w** and **s** fields needed to numerically solve eq 35. However, an irregularly shaped particle or even a sphere containing a noncentrosymmetric charge distribution poses greater difficulty. First of all, there is the problem of detemining the center of rotation, **d**. Garcia de la Torre and Bloomfield[14] have argued that this corresponds to the point at which the intrinsic viscosity (or equivalently ξ) is a minimum. For uncharged particles of arbitrary shape, they derive numerical equations that allow one to determine **d**. Subsequently, Garcia Bernal and Garcia de la Torre[15] discussed the example of an uncharged bent rod, and their Figure 2 (lower panel) shows how the intrinsic viscosity varies as the assumed center of rotation varies. In this particular example, the dependence of $[\eta]$ on **d** is fairly weak. Consequently, we expect that as long as one is close to the true center of rotation, the error introduced by being off in the choice of **d** should be small. In the present work, where our models are spheres containing simple charge distributions or capped cylinder models, we feel confident that the "center of mass" of our model and **d** should either coincide or be very close. Consequently, we shall not concern ourselves with actually determining **d** for the model polyions studied here. For model polyions of arbitrary shape such as protein models derived from crystal structures, **d** can be computed for uncharged model structures,[14,15] but the corresponding problem for charged structures merits further study. The complication that arises with polyions that is not a problem for uncharged macromolecules is that the **s**'s as well as the **w**'s depend on the choice of **d**. A second problem is that for particles in general, it is necessary to average over all possible particle orientations. Since the velocity field will be different for different particle orientations and since different orientations will have different **w**'s and **s**'s, it is clear that we are going to have to carry out a number of BE calculations in different orientations, or equivalently, a number of different shear field orientations for a given particle conformation, to properly evaluate eq 35. This problem is addressed in Appendix A and the principal results are summarized by eqs A17−A19. Basically, it is shown that the averaging procedure requires solving the BE problem for five different elementary shear configurations by holding the particle orientation constant. From eqs A17−A19, it might at first appear that ξ is independent of the choice of **d**. Keep in mind, however, that the shear field, $\mathbf{v}_0^{(l)}(\mathbf{y})$ and consequently $\mathbf{s}^{(l)}$ and $\mathbf{w}^{(l)}$ (where the "(l)" superscript refers to one of five elementary shear configurations) will depend on its choice and this will influence ξ.

One last point to address before discussing specific results concerns the importance of ion relaxation in influencing the viscosity. Consider the quantity

$$\xi_{\alpha\beta}{}'^{(l)} = -\frac{1}{\eta_0\gamma V_p}\left[\int_{S_p}\mathbf{r}\cdot\boldsymbol{P}_{\alpha\beta}\cdot\mathbf{w}'^{(l)}\,dS_y + \int_{\Omega}\mathbf{r}\cdot\boldsymbol{P}_{\alpha\beta}\cdot\mathbf{s}'^{(l)}\,dV_y\right] \quad (41)$$

where $\mathbf{r} = \mathbf{y} - \mathbf{d}$. This is equivalent to eq A17 except that auxiliary forces $\mathbf{s}'$ and $\mathbf{w}'$ are used instead of **s** and **w**. Using the relationships betwen primed and unprimed quantities (eqs 26 and 27), and shifting the origin of our integration domains, we find

$$\xi_{\alpha\beta}{}^{(l)} = \xi_{\alpha\beta}{}'^{(l)} - \frac{1}{\eta_0\gamma V_p}\left[\int_{S_p}\pi^{(l)}\mathbf{r}\cdot\boldsymbol{P}_{\alpha\beta}\cdot\mathbf{n}\,dS_r + \int_{\Omega}\mathbf{r}\cdot\boldsymbol{P}_{\alpha\beta}\cdot\nabla\pi^{(l)}\,dV_r\right] \quad (42)$$

Applying the divergence theorem to the term in brackets gives

$$\xi_{\alpha\beta}{}^{(l)} = \xi_{\alpha\beta}{}'^{(l)} + \frac{\delta_{\alpha\beta}}{\eta_0\gamma V_p}\int_{\Omega}\pi^{(l)}(r)\,dV_r - \frac{1}{\eta_0\gamma V_p}\int_{S_o}\pi^{(l)}\mathbf{r}\cdot\boldsymbol{P}_{\alpha\beta}\cdot\mathbf{n}\,dS_r \quad (43)$$

where $\delta_{\alpha\beta}$ is the Kronecker delta. Now the second term on the rhs of eq 43 only enters in the diagonal terms ($\alpha = \beta$) and from eq A19, these only appear for the $l =$ 4 and 5 terms. However, it is also clear from eq A19 that these terms cancel in calculating ξ. The third term on the rhs of eq 43 involves a surface integral over the outermost shell, S_o, which encloses the polyion and a relatively large volume of fluid. This term can be made negligible by setting S_o far from the polyion. It has been our observation, however, that this term falls off slowly as S_o is moved further out and that it should not be neglected in practice. In the absence of relaxation it does vanish to a good approximation. Hence, with the exception of this small correction, it is permissable to use the $\xi_{\alpha\beta}{}'^{(l)}$ terms to compute ξ.

From the discussion following eqs 26 and 27, we can identify $\mathbf{w}'^{(l)}$ with the hydrodynamic stress force on our particle in ambient shear field given by eqs A1 and A2 and effective external force field $\mathbf{s}'^{(l)}$. Now, in the absence of ion relaxation, $\mathbf{s}'^{(l)} = \mathbf{0}$ and so the problem is equivalent to the corresponding uncharged polyion. We can thus conclude that ξ (and consequently the intrinsic viscosity) for a polyion in the absence of ion relaxation is equal to that of the corresponding uncharged particle.

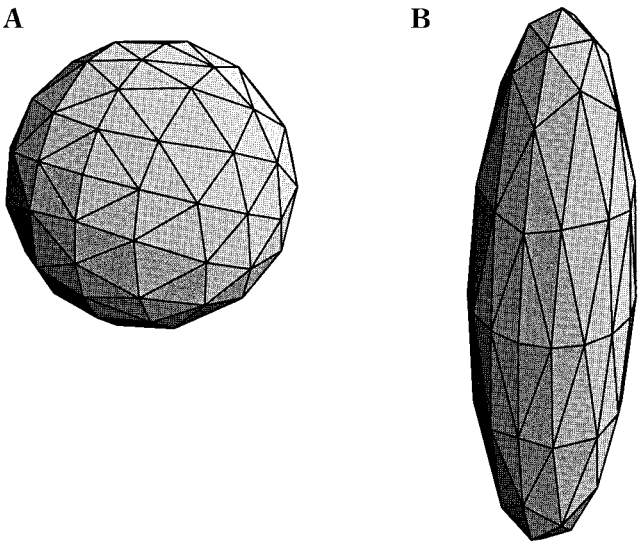

Figure 1. Surface models for sphere and prolate ellipsoid. The sphere, A, is made up of $N = 160$ platelets and is used in the calculation of the electroviscous effect of charged spheres. The prolate ellipsoid ($p = 4$) model is made up of 128 platelets.

Results

In the present work, our particles are modeled as plated structures and Figure 1 shows some representa-

Table 1. Viscosity Factors for Uncharged Prolate Ellipsoids

p	ξ[32]	ξ(BE)	relative error
1	2.500	2.447	−0.021
2	2.908	2.854	−0.019
3	3.685	3.704	+0.005
4	4.663	4.760	+0.021
6	7.098	7.273	+0.025
8	10.103	10.253	+0.015
10	13.634	13.537	−0.007

tive examples for a sphere (A) and ellipsoid (B). As an initial test of the BE methodology, it is applied to the problem of calculating viscosity factors, ξ's, for uncharged prolate ellipsoids. The particle is modeled as a rigid structure made up of 128 triangular plates and Figure 1B displays an example for a prolate ellipsoid with p = major axis/minor axis = 4. In one respect, this is a relatively simple case since the whole problem of ion relaxation is bypassed. As discussed in the previous section and Appendix A, however, it is necessary to carry out an average over five distinct particle orientations or shear field orientations in order to estimate ξ for an irregularly shaped particle. Thus, this example can be considered a test of the averaging procedure. Table 1 compares actual ξ's taken from Tables 10-2 of ref 32 with the BE values. In all cases, the BE calculations are accurate to within a few percent. Better agreement can be achieved by increasing the number of platelets used in the BE model. It should be kept in mind, however, that computation time varies roughly as the square of the number of platelets. As discussed in the Introduction, the general problem of the viscosity of uncharged particles of arbitrary shape has been thoroughly developed for models in which the structure is represented as an array of beads.[12−14] At first glance, it may appear that the BE methodology presented here (and Appendix A in particular) has little in common with the bead theories. It can be shown, however, that the BE expressions for ξ and intrinsic viscosity reduce to those of the bead theories under the appropriate conditions. This subject is addressed in Appendix B.

A spherical particle containing a single charge is examined next, and the results can be compared with the predictions of Booth[16] and Sherwood.[19] We shall consider a 2 nm sphere in 0.11 M monovalent salt for which $b = \kappa a = 2.18$ where κ is the Debye−Huckel screening parameter and a is the polyion radius. Co- and counterion mobilities or, equivalently, their diffusion constants, D_α, need to be specified as well. They can be related to limiting molar ionic conductivities, λ_α^∞, via the Nernst−Einstein relationship[34]

$$D_\alpha = \frac{\lambda_\alpha^\infty k_B T}{N_{Av} q^2 z_\alpha{}^2} \tag{44}$$

We shall use $\lambda_\alpha^\infty = 75.0 \times 10^{-4}$ S m^2/mol, appropriate for KCl.[34] In the BE calculation, the spherical polyion is represented as a geodesic surface made up of N platelets where N ranges from 96 to 384. Figure 1A gives an example with $N = 160$. The space surrounding the polyion is subdivided into J shells and each shell, in turn, is subdivided into N volume elements that resemble truncated pyramids. The inner face of the innermost shell corresponds to the actual polyion surface and the thickness of the shell varies as one moves outward. The outer face of the outermost shell is chosen to be at a distance d from the nearest point of the polyion surface, and this distance typically equals $16/\kappa$. In the calculations reported in this work, J is set to 50 throughout. Summarized in Table 2 are the results of 10 BE calculations in which a number of parameters are varied. Q_t represents the net charge (in protonic units), $y_0 = q\varsigma/k_BT$ where ς is the average surface or zeta potential, which is computed in the BE procedure, ξ_0 and ξ refer to the viscosity factors in the absence and presence of ion relaxation, and

Table 2. Spherical Polyions Containing a Single Central Charge

run	N	Q_t	y_0	κd	**v**-option	ξ_0	ξ	ϕ
1	96	−40	−3.432	16	u	2.447	2.688	0.098
2	128	−40	−3.440	8	u	2.459	2.710	0.102
3	128	−40	−3.441	12	u	2.462	2.716	0.103
4	128	−40	−3.446	16	u	2.462	2.723	0.106
5	128	−40	−3.450	24	u	2.461	2.724	0.107
6	160	−40	−3.450	16	u	2.463	2.725	0.106
7	160	−40	−3.450	16	n	2.463	2.749	0.116
8	384	−40	−3.459	16	u	2.477	2.744	0.108
9	128	−100	−5.481	16	n	2.461	3.027	0.230
10	128	−100	−5.481	16	u	2.461	2.968	0.206

$$\phi = \frac{\xi - \xi_0}{\xi_0} \tag{45}$$

is a relative measure of the viscoelectric effect. The "**v**-option" has to do with how the velocity field, **v**, surrounding the polyion is treated. In general, ion relaxation perturbs **v** but this perturbation is expected to be small. In the work of Booth[16] and Sherwood[19] the assumption is made that **v** is adequately described by that of the polyion in a shear field in the absence of any ion relaxation. As discussed previously, an iterative approach is used in the BE procedure in which successive estimates of relevant quantities such as the Φ_α and **v** fields are updated by iteration. The Booth−Sherwood approximation regarding **v** can be made in the BE procedure by simply not updating **v** after its initial calculation. This corresponds to the "n" choice in the **v**-option. In the overall framework of the BE procedure, however, there is no difficulty (other than additional cost in computation time) in updating **v** along with other quantities, and this corresponds to the "u" choice in the **v**-option.

Consider first runs 1, 4, 6, and 8 where N is varied but other parameters are held constant and $Q_t = -40$. It is evident from these results that ϕ shows only a weak dependence on the number of platelets in the model when we are trying to represent a sphere. In this case, it would appear that ϕ would extrapolate to about 0.110 in the limit of large N. From runs 2−5, where κd varies but other parameters are held constant, it is seen that ϕ changes only slightly as d increases. On this basis, we shall set $\kappa d = 16$ throughout the remainder of this work. From the BE calculations (with **v** updated) we conclude that ϕ is coming out around 0.110 when $Q_t = -40$, $a = 2$ nm, and the aqueous salt solution is 0.11 M KCl at 20 °C. From Booth's work,[16] we expect

$$\phi_B = q^* y_0{}^2 Z(b)(1 + b)^2 = q^* y_0{}^2 f(b) \tag{46}$$

where (for equal co- and counterion mobilities)

$$q^* = \frac{\epsilon_0 D_\alpha}{\eta_0 q^2} \tag{47}$$

and ϵ_o is the solvent dielectric constant (set to 78 in this work). Under the chosen working conditions, $q^* = 3.21$. Now $Z(b)$ (or $f(b)$) is a complicated function of b defined, and presented graphically, in Booth's paper.[16] When $b = 2.18$, $f(b)$ equals 0.003 67. For $y_0 = -3.45$ (computed from the BE calculation of Λ_0 for a geodescic sphere averaged over the surface), $\phi_B = 0.140$, which is somewhat larger than the BE value. It should be pointed out, however, that Booth's work is strictly limited to small absolute values of y_0. Sherwood[19] extended this to large values of $|y_0|$ and Figure 11 of ref 19 shows how the Booth values should be corrected depending on b and y_0. On the basis of this figure, we conclude that ϕ_B should overestimate ϕ by about 10% for $b = 2.18$ and $y_0 = -3.45$, and this leads to an estimate of ϕ of 0.126 that is slightly larger than the BE value of 0.110. Now Sherwood, in turn, assumes **v** is unperturbed by ion relaxation, but this corresponds to BE run number 7, which gives a ϕ value about 10% higher than the corresponding run in which **v** is updated (run 6). Thus, the BE value of 0.110 should be scaled upward by 10% (to give about 0.120) if we neglect the perturbation of **v** and this now agrees very well with Sherwood's prediction. For $Q_t = -100$, eq 46 gives $\phi_B = 0.354$, but from Figure 11 of Sherwood, this should be scaled by 0.65−0.70, which predicts ϕ in the range 0.230−0.248. This, however, is in very good agreement with BE run 9 in which **v** is not updated. As before, however, updating **v** reduces the ϕ obtained in the BE calulation by about 10% (run 10). Taking these various factors into consideration, we conclude that electroviscous effects predicted by the BE method are in very good agreement with existing theory for this particular example. They also show that neglecting the perturbation of **v** leads to an overestimate in the electroviscous effect by about 10% in the few cases studied here.

Before leaving the subject of spherical model polyions, two additional examples shall be considered that contain more complicated (noncentrosymmetric) charge distributions. We shall choose $a = 2$ nm, 0.11 M KCl, and $N = 160$. In the "dipolar" case, charges ±40 are placed inside the sphere at coordinates (±1 nm, 0, 0) where the sphere center is chosen to coincide with the origin of our reference frame. In the "quadrupolar" case, charges −40 are placed at (±1 nm, 0, 0) and an additional +80 charge is placed at the origin. It should be pointed out that the net charge of the dipolar and quadrupolar cases is zero. Because of the more complex charge distributions, it is necessary to average over different elementary shear configurations. Now ϕ for the "monopole" (run number 6 in Table 2), dipole, and quadrupole cases turn out to be 0.106, 0.077, and 0.031, respectively. Although the dipolar and quadrupolar cases have somewhat smaller ϕ's than for the monopole, they are of comparable size and show that the viscoelectric effect depends not only on a polyion's net charge, but on how that charge is distributed within. In free solution electrophoresis of spherical polyions, the mobility depends strongly on the net charge (monopole) but relatively weakly on the charge distribution. In particular, the electrophoretic mobility is independent of its (charge) dipole moment.[21,35,36] From the present study, it is clear that electroviscous effects do depend on the dipole moment and, although more weakly, on higher charge moments as well. Although the dipole moment considered in the example above is very large, it should be mentioned that biomolecules with large dipole moments do exist in nature. Examples include cytochromes,[37,38] acetylcholinesterases,[39] and certain endonucleases.[40]

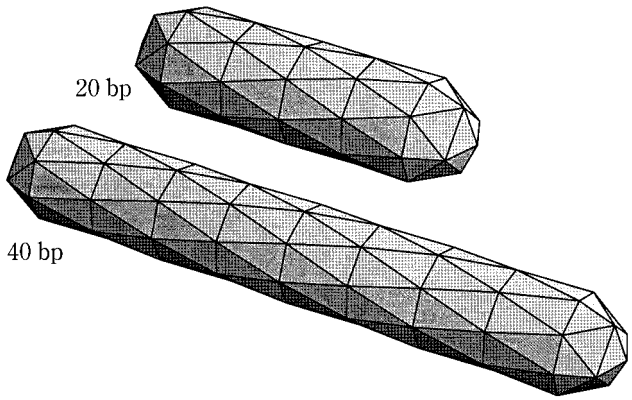

Figure 2. Surface models for DNA fragments. The 20 bp model has $N = 96$ in this example, while the 40 bp model has $N = 160$.

Table 3. 20 bp DNA in 0.11 M KCl

N	ξ_0	ξ	ϕ
72	3.898	4.211	0.080
96	4.004	4.349	0.086
120	4.018	4.366	0.087

Next, we shall apply the BE methodology to models of short DNA fragments. DNA is a highly charged polyanion with −2 charges per base pair and a base pair length of 0.34 nm. In the present work, this charge distribution is modeled as a double helical spiral with the spirals situated 0.60 nm from the helix axis. The value of 0.60 nm is chosen instead of an average structural value of 0.90 nm[32] to reduce tangential gradients in Λ_o. Consistent with closely related work on electrophoresis,[23] electroviscosities do not depend strongly on the details of the charge distribution. Charges of −1 are placed on these spirals every 0.34 nm along the helix axis and the pitch of the spirals are 3.4 nm per turn. As in previous modeling studies of the electrophoretic mobility,[23] capped cylinder models are used to represent the DNAs in the present work and some of these are illustrated in Figure 2. Since crystal structures are not available for fragments of this length, the structures are designed to reproduce the translational and rotational diffusional constants and can be likened to right circular cylinders with an axial radius of 1.0 nm and a length of $0.34N_{bp}$ nm where N_{bp} is the number of base pairs.[41,42] Shown in Table 3 are viscosity data for 20 bp DNA in 0.11 M KCl, $\kappa d = 16$, and variable N. The reduced surface potential, y_0, is about −3.44 and is nearly independent of N. This value is almost identical to the 2 nm sphere in the same salt solution with the same net charge of −40. On the basis of these results, we conclude that a simple surface made up of about 100 platelets is adequate to model the viscosity of this particular polyion. The ξ values are substantially larger than the corresponding values of the sphere, which is due to the different shapes of the two models. Comparing the ξ_0's in Table 3 with those of the (uncharged) prolate ellipsoids in Table 1, it is clear that the capped cylinder model exhibits the viscosity behavior of a prolate ellipsoid with p between 3 and 4. The viscoelectric factor ϕ is somewhat smaller for 20 bp DNA than a 2 nm sphere containing the same net charge (and nearly the same y_0). As discussed previously, the viscoelectric effects are computed by an

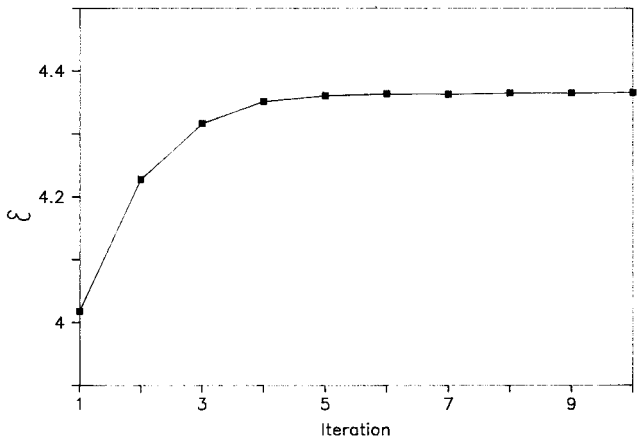

Figure 3. ξ versus iteration number for 20 bp DNA. In this example, the salt concentration is 0.11 M and $N = 120$.

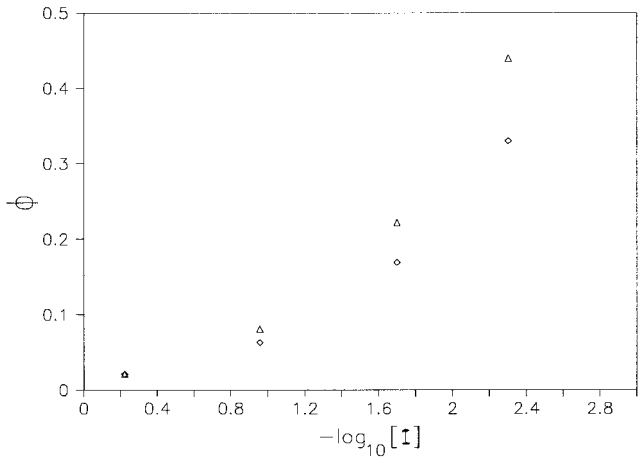

Figure 4. ϕ versus salt concentration for 20 and 40 bp DNA. In all cases $N = 96$ for 20 bp and $N = 160$ for 40 bp studies. Also $\xi_0 = 4.00$ and 8.04 for 20 and 40 bp models, respectively. Triangles/diamonds correspond to 20/40 bp fragments.

iterative BE procedure in which physical quantities such as the **v** and Φ_α fields are updated until convergence is achieved. Shown in Figure 3 is ξ versus iteration number for the $N = 120$, 20 bp DNA run.

It is expected that the primary electroviscous effect depends strongly on the ambient salt concentration since both Λ_0 and the "thickness" of the ion atmosphere are influenced by it. Plotted in Figure 4 is ϕ versus −log [I] (where I is the monovalent salt concentration in mol/liter) for both 20 and 40 bp DNA fragments. At high salt concentration, the electroviscous effect goes to zero but at low salt, it can be substantial. In the above example, the monovalent salt is KCl, though other salts with different ion mobilities can be considered. In a final example, we consider 20 bp DNA ($N = 96$) in 0.02 M Tris−acetate. Limiting molar conductivities of 29.7 $\times 10^{-4}$ (S m^2)/mol for Tris[43] and 40.8 $\times 10^{-4}$ (S m^2)/mol for acetate[44] were used in eq 44 to estimate the ion diffusion constants. In this case, $\phi = 0.494$, which is substantially larger than the value of 0.222 found with KCl. Since Tris is a bulkier counterion than K^+, the extent of ion relaxation, and consequently the viscoelectric effect, is expected to be greater for Tris than K^+ under otherwise identical conditions. These results are qualitatively consistent with expectations for spherical polyions on the basis of the Booth[16] and Sherwood[17] theories.

Summary

In this work, a numerical boundary element (BE) procedure has been developed to predict intrinsic viscosities and related quantities of dilute, rigid model macromolecules of arbitrary shape and charge distribution. For uncharged macromolecules, the BE procedure predicts intrinsic viscosities in perfect agreement with the bead theories.[14,45] However, the primary objective has been to account for the effects of ion relaxation on the viscosity of charged macromolecules. For the special case of a spherical polyion containing a centrosymmetric charge distribution, the BE results are in excellent agreement with the predictions of Sherwood.[19] Actually, the BE approach applied to the sphere goes beyond earlier work by including the effect of ion relaxation on the fluid velocity field in the vicinity of the polyion, which was left out of previous work. Accounting for this reduces the viscoelectric effect by about 10% for the examples considered here. In addition to a centrosymmetric charge distribution for spherical model polyions, dipolar and quadrupolar charge distributions are also considered. These show that the electroviscous effects depend on charge distribution (dipole, quadrupole) as well as net charge. The BE approach is then applied to short DNA fragments in the range of 0.005−0.6 M monovalent salt where the electroviscous effect ranges from about 45% (20 bp) and 30% (40 bp) at low salt down to about 2% (20 and 40 bp) at high salt. Most viscosity studies appearing in the literature deal with high molecular weight polyelectrolytes where secondary and tertiary viscoelectric effects dominate.[5,46,47] It is hoped that the present study will stimulate further experimental work on the subject of the primary electroviscous effect of dilute, rigid macromolecules. The case study of the 20 and 40 bp DNA fragments shows that the effect is predicted to be large enough to observe.

Appendix A: Averages for the General Problem

Let us assume we have a simple shear field characterized by one of the following five elementary shear fields far from the particle

$$\mathbf{v}_0^{(l)}(\mathbf{y}) = \frac{1}{2}\boldsymbol{E}^{(l)}\cdot(\mathbf{y} - \mathbf{d}) \tag{A1}$$

where **d** is the center of rotation and

$$\boldsymbol{E}^{(1)} = \gamma(\mathbf{e}_1\mathbf{e}_2 + \mathbf{e}_2\mathbf{e}_1) \tag{A2a}$$

$$\boldsymbol{E}^{(2)} = \gamma(\mathbf{e}_1\mathbf{e}_3 + \mathbf{e}_3\mathbf{e}_1) \tag{A2b}$$

$$\boldsymbol{E}^{(3)} = \gamma(\mathbf{e}_2\mathbf{e}_3 + \mathbf{e}_3\mathbf{e}_2) \tag{A2c}$$

$$\boldsymbol{E}^{(4)} = \gamma(\mathbf{e}_1\mathbf{e}_1 - \mathbf{e}_2\mathbf{e}_2) \tag{A2d}$$

$$\boldsymbol{E}^{(5)} = \gamma(\mathbf{e}_1\mathbf{e}_1 - \mathbf{e}_3\mathbf{e}_3) \tag{A2e}$$

where $\mathbf{e}_\alpha$ is a unit vector along the αth axis of some convenient laboratory fixed frame (Σ). Now immerse our particle in the fluid characterized by one of these elementary shear fields and denote the velocity, pressure, and external force per unit volume fields by $\mathbf{v}^{(l)}$, $p^{(l)}$, and $\mathbf{s}^{(l)}$, respectively. These fields satisfy the Navier−Stokes and solvent incompressibility equations given by eqs 14 and 15 subject to the boundary conditions $\mathbf{v}^{(l)} \rightarrow \mathbf{0}$ on the particle surface and $\mathbf{v}^{(l)} \rightarrow \mathbf{v}_0^{(l)}$ far

away from the particle surface. As described in the body of the present work, the BE approach can be used to solve these five problems.

Now suppose we have an arbitrary shear field, $\mathbf{v}_0$, (see eqs 36 and 37) and that we decompose this as a superposition of our elementary shear fields

$$\mathbf{v}_0(\mathbf{y}) = \frac{1}{2}\boldsymbol{E}\cdot(\mathbf{y} - \mathbf{d}) = \sum_{l=1}^{5} c^{(l)}\mathbf{v}_0{}^{(l)}(\mathbf{y}) \tag{A3}$$

Let $\mathbf{v}(\mathbf{y})$ represent the solution of eqs 14 and 15 subject to the appropriate boundary conditions. Can we write $\mathbf{v}$ as a simple superposition of the $\mathbf{v}^{(l)}$? Consider the difference fields

$$\Delta\mathbf{v} = \mathbf{v} - \sum_l c^{(l)}\mathbf{v}^{(l)} \tag{A4a}$$

$$\Delta p = p - \sum_l c^{(l)}p^{(l)} \tag{A4b}$$

and the Navier−Stokes equation for the difference fields are

$$\eta_0\nabla^2\Delta\mathbf{v} - \nabla\Delta p = -(\mathbf{s} - \sum_l c^{(l)}\mathbf{s}^{(l)}) \tag{A5}$$

and $\Delta\mathbf{v} \rightarrow \mathbf{0}$ at the particle surface and at infinity. Since we are restricting ourselves to perturbations that are linear in the shear field, we can also write $\mathbf{s}$ as a superposition of the $\mathbf{s}^{(l)}$

$$\mathbf{s}(\mathbf{y}) = \sum_l c^{(l)}\mathbf{s}^{(l)}(\mathbf{y}) \tag{A6}$$

It is then clear that a particular solution to eq A5 is $\Delta\mathbf{v} = \mathbf{0}$ and $\Delta p = 0$. Furthermore, from Theorem 4 of Chapter II of Ladyzhenskaya,[26] we can conclude that this null solution is also the unique solution. Hence, we can write

$$\mathbf{v}(\mathbf{y}) = \sum_{l=1}^{5} c^{(l)}\mathbf{v}^{(l)}(\mathbf{y}) \tag{A7}$$

and the geometry of the shear field determines the $c^{(l)}$'s. From the transformation properties of Cartesian second rank matrixes,[48] we can write

$$\boldsymbol{E} = \boldsymbol{A}\cdot\boldsymbol{E}^{(1)}\cdot\boldsymbol{A}^{\mathrm{T}} \tag{A8}$$

where $\mathbf{A}$ is the transformation matrix that carries a reference frame in which the shear field is described by $\mathbf{E}^{(1)}$ (Σ') into one described by $\mathbf{E}$ (Σ) and the "T" superscript denotes transpose. The matrix $\mathbf{A}$, in turn, can be defined in terms of three Euler angles (ψ, θ, ϕ)[14] and elementary rotation matrices $\mathbf{R}_z$ and $\mathbf{R}_x$[48]

$$\boldsymbol{A}(\psi,\theta,\phi) = \boldsymbol{R}_z(\psi)\cdot\boldsymbol{R}_x(\theta)\cdot\boldsymbol{R}_z(\phi) \tag{A9}$$

where

$$\boldsymbol{R}_z(\phi) = \begin{pmatrix} \cos\phi & \sin\phi & 0 \\ -\sin\phi & \cos\phi & 0 \\ 0 & 0 & 1 \end{pmatrix};$$

$$\boldsymbol{R}_x(\theta) = \begin{pmatrix} 1 & 0 & 0 \\ 0 & \cos\theta & \sin\theta \\ 0 & -\sin\theta & \cos\theta \end{pmatrix} \tag{A10}$$

The unit vectors $\mathbf{e}_a$ and $\mathbf{e}_b$ (see discussion following eq 29) can be written

$$\mathbf{e}_a = \sum_{\alpha=1}^{3} A_{\alpha 1}\mathbf{e}_\alpha \tag{A11a}$$

$$\mathbf{e}_b = \sum_{\alpha=1}^{3} A_{\alpha 2}\mathbf{e}_\alpha \tag{A11b}$$

It is straightforward to express the $c^{(l)}$ coefficients in terms of the A_{ij}'s.

$$c^{(1)} = A_{12}A_{21} + A_{11}A_{22} \tag{A12a}$$

$$c^{(2)} = A_{12}A_{31} + A_{11}A_{32} \tag{A12b}$$

$$c^{(3)} = A_{22}A_{31} + A_{21}A_{32} \tag{A12c}$$

$$c^{(4)} = -2A_{22}A_{21} \tag{A12d}$$

$$c^{(5)} = -2A_{31}A_{32} \tag{A12e}$$

Inserting eq A11 into eq 35 and discretizing the surface and volume integrations following eqs 19−22 yield

$$\xi = \frac{1}{\eta_0\gamma V_{\mathrm{p}}}[\sum_{j,\alpha,\beta}\langle A_{\alpha 1}A_{\beta 2}w_{j\alpha}r_{j\beta}\rangle + \sum_{k,\alpha,\beta}\langle A_{\alpha 1}A_{\beta 2}s_{k\alpha}r_{k\beta}\rangle] \tag{A13}$$

where the sum over j/k extends over all surface/volume elements and the sum over α and β is from 1 to 3. Also in eq A13, we have defined $\mathbf{r}_i = \mathbf{y}_i - \mathbf{d}$. On the basis of eq 34, it might at first appear that we could use any arbitrary position vector, $\mathbf{c}$, instead of the center of rotation, $\mathbf{d}$, in eq A13 and indeed this is correct. However, since we need to average this over all possible particle orientations, only the projection, $\mathbf{y}_i - \mathbf{d}$ will remain. Hence the substitution of $\mathbf{d}$ for $\mathbf{c}$ in eq A13. Before averaging the above equation over all possible orientations, it is important to remember that $\mathbf{s}$ and $\mathbf{w}$ also depend on orientation. From eq A6 and an entirely analogous relation for $\mathbf{w}$,

$$\xi = -\frac{1}{\eta_0\gamma V_{\mathrm{p}}}\sum_{l,\alpha,\beta}\langle A_{\alpha 1}A_{\beta 2}c^{(l)}\rangle[\sum_j w_{j\alpha}{}^{(l)}r_{j\beta} + \sum_k s_{k\alpha}{}^{(l)}r_{k\beta}] \tag{A14}$$

Averaging the quantity in brackets over Euler angles can now be carried out. Defining

$$(\boldsymbol{C}^{(l)})_{\alpha\beta} = \langle A_{\alpha 1}A_{\beta 2}c^{(l)}\rangle \tag{A15}$$

it can be shown

$$\gamma \boldsymbol{C}^{(1)} = \frac{1}{10}\boldsymbol{E}^{(1)} \tag{A16a}$$

$$\gamma \boldsymbol{C}^{(2)} = \frac{1}{10}\boldsymbol{E}^{(2)} \tag{A16b}$$

$$\gamma \boldsymbol{C}^{(3)} = \frac{1}{10}\boldsymbol{E}^{(3)} \tag{A16c}$$

$$\gamma \boldsymbol{C}^{(4)} = \frac{2}{15}\boldsymbol{E}^{(4)} - \frac{1}{15}\boldsymbol{E}^{(5)} \tag{A16d}$$

$$\gamma \boldsymbol{C}^{(5)} = \frac{2}{15}\boldsymbol{E}^{(5)} - \frac{1}{15}\boldsymbol{E}^{(4)} \tag{A16e}$$

Also define

$$\xi_{\alpha\beta}{}^{(l)} = -\frac{1}{\eta_0 \gamma V_p}\left[\sum_j r_j \cdot \boldsymbol{P}_{\alpha\beta} \cdot \mathbf{w}_j{}^{(l)} + \sum_k r_k \cdot \boldsymbol{P}_{\alpha\beta} \cdot \mathbf{s}_k{}^{(l)}\right] \tag{A17}$$

where

$$\boldsymbol{P}_{\alpha\beta} = \frac{1}{2}(\boldsymbol{e}_\alpha \boldsymbol{e}_\beta + \boldsymbol{e}_\beta \boldsymbol{e}_\alpha) \tag{A18}$$

From eqs A15−A18, eq A14 can be put into the final form

$$\xi = \frac{1}{5}(\xi_{12}{}^{(1)} + \xi_{13}{}^{(2)} + \xi_{23}{}^{(3)}) + \frac{1}{15}(\xi_{11}{}^{(4)} + \xi_{33}{}^{(4)} - 2\xi_{22}{}^{(4)} + \xi_{11}{}^{(5)} + \xi_{22}{}^{(5)} - 2\xi_{33}{}^{(5)}) \tag{A19}$$

Appendix B: Connection with (Uncharged) Bead Models

In the absence of external forces, eq 35 can be written

$$\xi = -\frac{1}{\eta_0 \gamma V_p}\sum_{i=1}^{N}\langle \mathbf{w}_{ia}(\mathbf{y}_i - \mathbf{d})_b\rangle \tag{B1}$$

where the surface has been discretized into N "elements" and the assumption has been made that the force per unit area exerted by the particle on the surrounding fluid is constant, to a good approximation, over a given element. In eq B1, $\mathbf{w}_i$ is the net force exerted by element *i* on the fluid and **d** is the center of rotation. As discussed in Appendix A, we can replace an arbitrary position vector, **c**, with **d** since orientational averaging effectively reduces eq 35 to this case. The term "particle" in this appendix refers to the entire structure being modeled. In the boundary element approach, it is convenient to model the elements as a series of interlocking plates, as shown in Figure 1. In general, however, alternative models can be employed. It is possible, for example, to represent a globular protein as a shell of small beads that act as centers of frictional resistance in calculating its transport properties.[14,45,49] This "extrapolated shell model"[49] has been extensively used in biophysics.[45] The origin of this approach, in turn, can be traced to Kirkwood and co-workers who applied "bead models" to a variety of problems including a theory for the viscosity of linear chain molecules.[11] Because bead methods have been extensively used yet the connection between the bead and BE methods may not be transparent, we felt it was appropriate to show how the BE treatment of viscosity reduces to those of the bead methods when the model particle is uncharged.

Thus, instead of modeling the elements of our particle as a series of plates, model them as beads instead with $\mathbf{y}_i$ in eq B1 corresponding to the position of the center of bead *i*. Also replace $\mathbf{w}_i$ with $\mathbf{F}_i$ (the force exerted by bead *i* on the solvent) simply to be more consistent with the notation in the existing literature.[45] Using eq 34 in eq B1 with the notational change mentioned above

$$[\eta] = -\frac{N_{Av}}{\eta_0 \gamma M}\sum_i \langle \mathbf{F}_{ia}(\mathbf{y}_i - \mathbf{d})_b\rangle \tag{B2}$$

which is the standard starting expression for the intrinsic viscosity in many applications.[11−14] To evaluate eq B2 for $[\eta]$ or a very similar relation for ξ using the formalism described in Appendix A, use is made of eqs A17 and A18

$$\xi_{\alpha\beta}{}^{(l)} = -\frac{1}{2\eta_0 \gamma V_p}\sum_i (\mathrm{r}_{i\alpha}\mathrm{F}_{i\beta}{}^{(l)} + \mathrm{r}_{i\beta}\mathrm{F}_{i\alpha}{}^{(l)}) \tag{B3}$$

where

$$\mathbf{r}_i = \mathbf{y}_i - \mathbf{d} \tag{B4}$$

and $\mathbf{F}_i{}^{(l)}$ is the force exerted by bead *i* on the fluid for our particle placed in elementary shear field "*l*" (eqs A1 and A2). Starting with eq 40, setting $\mathbf{s} = \mathbf{0}$ and assuming **w** is constant over each bead comprising our entire particle, one can show that

$$\langle \mathbf{v}_i{}^{(l)}\rangle = \mathbf{v}_{i0}{}^{(l)} + \sum_{j\neq i} \boldsymbol{T}_{ij} \cdot \mathbf{F}_j{}^{(l)} \tag{B5}$$

where $\mathbf{T}_{ij}$ is the Rotne−Prager[50] or modified Oseen tensor described elsewhere,[45] and $\mathbf{v}_{i0}{}^{(l)}$ is the velocity the fluid would have at $\mathbf{y}_i$ if the (entire) particle were absent. The quantity $\langle \mathbf{v}_i\rangle$ is the fluid velocity averaged over the entire surface of bead *i* if bead *i* were removed (but all other beads remained). To derive eq B5 from eq 40 it is necessary to expand **U** (in eq 40) about $\mathbf{y}_i - \mathbf{y}_j$ to second order and average over the surfaces of both beads *i* and *j*. In the bead model approaches, the forces are related to the velocities via[11,45]

$$\mathbf{F}_i{}^{(l)} = \varsigma_i(\mathbf{u}_i - \langle \mathbf{v}_i{}^{(l)}\rangle) \tag{B6}$$

where ς_i is the friction factor for bead *i* and $\mathbf{u}_i$ is the actual velocity of bead *i*. In the present application $\mathbf{u}_i = \mathbf{0}$. If we define

$$\boldsymbol{Q}_{ij} = \delta_{ij}\boldsymbol{I} + (1 - \delta_{ij})\varsigma_i \boldsymbol{T}_{ij} \tag{B7}$$

it is possible to express eq B5 as

$$\sum_j \boldsymbol{Q}_{ij} \cdot \mathbf{F}_j{}^{(l)} = -\frac{\varsigma_i}{2}\boldsymbol{E}^{(l)} \cdot (\mathbf{y}_i - \mathbf{d}) \tag{B8}$$

Now it is straightforward to solve eq B8 for $\mathbf{F}_i{}^{(l)}$ using the same matrix inversion procedure used to solve for the $\mathbf{w}_i$'s (eq 25) except that 3×3 submatrices $\mathbf{S}_{ij}$ are part of the $3N \times 3N$ supermatrix **S**, which is the inverse of the $3N \times 3N$ supermatrix **Q**, which is made up of the N^2 3×3 submatrices $\mathbf{Q}_{ij}$. Inversion of eq B8 yields

$$\mathbf{F}_i{}^{(l)} = -\frac{1}{2}\sum_j \varsigma_j \boldsymbol{S}_{ij} \cdot \boldsymbol{E}^{(l)} \cdot (\mathbf{y}_j - \mathbf{d}) \tag{B9}$$

Inserting eq B9 into eq B3 gives

$$\xi_{\alpha\beta}^{(l)} = \frac{1}{4\eta_0\gamma V_p}\sum_{i,j=1}^{N}\sum_{\delta,\epsilon=1}^{3}\varsigma_j[r_{i\alpha}S_{ij}^{\beta\epsilon}E_{\epsilon\delta}^{(l)}r_{j\delta} + r_{i\beta}S_{ij}^{\alpha\epsilon}E_{\epsilon\delta}^{(l)}r_{j\delta}] \tag{B10}$$

Making use of eq B10 in eq A19 along with the definitions of the $\mathbf{E}^{(l)}$ given by eqs A2, it is straightforward to show

$$\xi = \sum_{i,j=1}^{N}\frac{\varsigma_j}{\eta_0 V_p}\left(\frac{1}{15}\sum_{\alpha}r_{i\alpha}S_{ij}^{\alpha\alpha}r_{j\alpha} + \frac{1}{20}\sum_{\alpha\neq\beta}r_{i\alpha}S_{ij}^{\beta\alpha}r_{j\beta} - \frac{1}{30}\sum_{\alpha\neq\beta}r_{i\alpha}S_{ij}^{\alpha\beta}r_{j\beta} + \frac{1}{20}\sum_{\alpha\neq\beta}r_{i\alpha}S_{ij}^{\beta\beta}r_{j\alpha}\right) \tag{B11}$$

Equation B11 is entirely consistent with eq 27 of Garcia de la Torre and Bloomfield,[14] who employed a somewhat different averaging approach than that used in Appendix A. Garcia de la Torre and Bloomfield go on to derive explicit expressions for the components of **d** by differentiating $[\eta]$ with respect to the components of **d** and setting the resultant equations to zero.

References and Notes

(1) Bull, H. B. *An Introduction to Physical Biochemistry*; F. A. Davis Co.: Philadelphia, PA, 1964; Chapter 13.
(2) Conway, B. E.; Dobry-Duclaux, A. In *Rheology: Theory and Applications*; Eirich, F. R., Ed.; Academic Press: New York, 1966; Vol. 3, p 83.
(3) Hunter, R. J. *Zeta Potential in Colloid Science*; Academic Press: New York, 1981; Chapter 5.
(4) Schmitz, K. S. *Macroions in Solution and Colloidal Suspension*; VCH Publishers: New York, 1993; Chapter 4.
(5) Imai, N.; Gekko, K. *Biophys. Chem.* **1991**, *41*, 31.
(6) Fixman, M.; Skolnick, J. *Macromolecules* **1978**, *11*, 863.
(7) Einstein, A. in *Investigations on the Theory of the Brownian Movement*; Furth, R., Ed.; Cowper, A. D., translator; Dover Publications: New York, 1956; Chapter 3.
(8) Jeffrey, G. B. *Proc. R. Soc. London* **1923**, *A102*, 161.
(9) Simha, R. *J. Phys. Chem.* **1940**, *44*, 25.
(10) Scheraga, H. A. *J. Chem. Phys.* **1955**, *23*, 1526.
(11) Kirkwood, J. G.; Riseman, J. *J. Chem. Phys.* **1948**, *16*, 565.
(12) McCammon, J. A.; Deutch, J. M. *Biopolymers* **1976**, *15*, 1397.
(13) Nakajima, H.; Wada, Y. *Biopolymers* **1977**, *16*, 875.
(14) Garcia de la Torre, J.; Bloomfield, V. A. *Biopolymers* **1978**, *17*, 1605.
(15) Garcia Bernal, J. M.; Garcia de la Torre, J. *Biopolymers* **1980**, *19*, 751.
(16) Booth, F. *Proc. R. Soc. London* **1950**, *A203*, 533.
(17) Russel, W. B. *J. Fluid Mech.* **1978**, *85*, 209.
(18) Lever, D. A. *J. Fluid Mech.* **1979**, *92*, 421.
(19) Sherwood, J. D. *J. Fluid Mech.* **1980**, *101*, 609.
(20) Wiersema, P. H.; Loeb, A. L.; Overbeek, J. Th. G. *J. Colloid Interface Sci.* **1966**, *22*, 78.
(21) Allison, S. A. *Macromolecules* **1996**, *29*, 7391.
(22) Allison, S. A.; Potter, M.; McCammon, J. A. *Biophys. J.* **1997**, *73*, 133.
(23) Allison, S. A.; Mazur, S. *Biopolymers*, in press.
(24) O'Brien, R. W.; White, L. R. *J. Chem. Soc., Faraday Trans. 2* **1978**, *74*, 1607.
(25) Zhou, H.-X. *J. Chem. Phys.* **1994**, *100*, 3152.
(26) Ladyzhenskaya, O. A. *The Mathematical Theory of Viscous Incompressible Flow*; Gordon and Breach, New York, 1963; Chapter 3.
(27) Kim, S.; Karilla, S. J. *Microhydrodynamics*; Butterworth-Heinemann: London, 1991; Chapter 2.
(28) Allison, S. A.; Nambi, P. *Macromolecules* **1994**, *27*, 1413.
(29) Zimm, B. H.; Crothers, D. M. *Proc. Natl. Acad. Sci. U.S.A.* **1962**, *48*, 905.
(30) Batchelor, G. K. *J. Fluid Mech.* **1970**, *41*, 545.
(31) Russel, W. B. *J. Colloid Interfac. Sci.* **1976**, *55*, 590.
(32) Cantor, C. R.; Schimmel, P. R. *Biophysical Chemistry*; W. H. Freeman: San Francisco, CA, 1980; Vol. 2.
(33) Van Holde, K. E. *Physical Biochemistry*; Prentice-Hall: Englewood Cliffs, NJ, 1971.
(34) Castellan, G. W. *Physical Chemistry*; 3rd ed.; Addison-Wesley: Reading, MA, 1983.
(35) Yoon, B. J. *J. Colloid Interface Sci.* **1991**, *142*, 575.
(36) Solomentsev, Y. E.; Pawar, Y.; Anderson, J. L. *J. Colloid Interface Sci.* **1993**, *158*, 1.
(37) Dixon, D. W.; Hong, X.; Woehler, S. E. *Biophys. J.* **1989**, *56*, 339.
(38) Koppenol, W. H.; Rush, J. D.; Mills, J. D.; Margoliash, E. *Mol. Biol. Evol.* **1991**, *8*, 545.
(39) Porschke, D.; Creminon, C.; Cousin, X.; Bon, C.; Sussman, J.; Silman, I. *Biophys. J.* **1996**, *70*, 1603.
(40) Antosiewicz, J.; Miller, M. D.; Krause, K. L.; McCammon, J. A. *Biopolymers* **1997**, *41*, 443.
(41) Eimer, W.; Pecora, R. *J. Chem. Phys.* **1991**, *94*, 2324.
(42) Fujimoto, B. S.; Miller, J. M.; Ribiero, N. S.; Schurr, J. M. *Biophys. J.* **1994**, *67*, 304.
(43) Klein, S. D.; Bates, R. G. *J. Solution Chem.* **1980**, *9*, 289.
(44) *Handbook of Chemistry and Physics*, 74th ed.; Lide, D. R., Ed.; CRC Press: Boca Raton, FL, 1993; pp 5-91, 92.
(45) Garcia de La Torre, J.; Bloomfield, V. A. *Q. Rev. Biophys.* **1981**, *14*, 81.
(46) Yamanaka, J.; Araie, H.; Matsuoka, H.; Kitano, H.; Ise, N.; Yamaguchi, T.; Saeki, S.; Tsubokawa, M. *Macromolecules* **1991**, *24*, 3206.
(47) Antonietti, M.; Briel, A.; Foerster, S. *J. Chem. Phys.* **1996**, *105*, 7795.
(48) Arfken, G. *Mathematical Methods for Physicists*, 2nd ed.; Academic Press: New York, 1970; Chapter 4.
(49) Teller, D. C.; Swanson, E.; de Haen, C. *Methods Enzymol.* **1979**, *61*, 103.
(50) Rotne, J.; Prager, S. *J. Chem. Phys.* **1969**, *50*, 4831.

MA980250O